NADPH oxidases regulate septin-mediated cytoskeletal remodeling during plant infection by the rice blast fungus

Lauren S. Ryder[a], Yasin F. Dagdas[a], Thomas A. Mentlak[a], Michael J. Kershaw[a], Christopher R. Thornton[a], Martin Schuster[a], Jisheng Chen[b], Zonghua Wang[b], and Nicholas J. Talbot[a,1]

[a]School of Biosciences, University of Exeter, Exeter EX4 4QD, United Kingdom; and [b]Department of Plant Protection, Fujian Agriculture and Forestry University, Fuzhou, Fujian 350002, China

Edited by Jay C. Dunlap, Dartmouth Medical School, Hanover, NH, and approved January 10, 2013 (received for review October 7, 2012)

The rice blast fungus *Magnaporthe oryzae* infects plants with a specialized cell called an appressorium, which uses turgor to drive a rigid penetration peg through the rice leaf cuticle. Here, we show that NADPH oxidases (Nox) are necessary for septin-mediated reorientation of the F-actin cytoskeleton to facilitate cuticle rupture and plant cell invasion. We report that the Nox2–NoxR complex spatially organizes a heteroligomeric septin ring at the appressorium pore, required for assembly of a toroidal F-actin network at the point of penetration peg emergence. Maintenance of the cortical F-actin network during plant infection independently requires Nox1, a second NADPH oxidase, which is necessary for penetration hypha elongation. Organization of F-actin in appressoria is disrupted by application of antioxidants, whereas latrunculin-mediated depolymerization of appressorial F-actin is competitively inhibited by reactive oxygen species, providing evidence that regulated synthesis of reactive oxygen species by fungal NADPH oxidases directly controls septin and F-actin dynamics.

pathogenicity | plant pathogen | tetraspanin | gelsolin | GTPase

NADPH oxidases (Nox) are flavoenzymes that function by transferring electrons across biological membranes to catalyze reduction of molecular oxygen to superoxide (1, 2). In animal cells, Nox enzymes are implicated in cell proliferation, cell signaling, and apoptosis (1–3), whereas in plants Nox are necessary for programmed cell death (4), the response to environmental stresses (4), pathogen infection (5), and polarized growth of root hairs (6). In filamentous fungi, Nox are necessary for cellular differentiation during sexual reproduction and for developmental processes that involve transitions from nonpolarized to polarized cell growth, such as tissue invasion by mutualistic and pathogenic fungi, and fungal virulence (7–9). The underlying function of Nox enzymes in these diverse developmental processes remains unclear.

In this study we set out to investigate the role of reactive oxygen species (ROS) synthesis by Nox during plant infection by the devastating rice blast pathogen *Magnaporthe oryzae* (10). Rice blast disease is considered a major threat to global food security and remains difficult to control (11). Nox1 and Nox2 are necessary for an oxidative burst that is required for plant infection by the fungus (12), but why this is necessary for rice blast disease is not known. To infect rice plants, *M. oryzae* forms a specialized infection structure called an appressorium (10). This dome-shaped cell generates enormous turgor of up to 8.0 MPa (12), which is translated into physical force at its base to rupture the rice leaf cuticle using a narrow, rigid, penetration peg that invades plant tissue. Recently, it has been reported that septin GTPases scaffold cortical F-actin in the appressorium at the site of plant infection, acting via the ezrin-radixin-moesin (ERM) protein, Tea1, and specific phosphatidylinoside interactions at the fungal plasma membrane (13). *M. oryzae* septins assemble into a hetero-oligomeric ring that surrounds the appressorium pore, a region at the base of the infection cell from which the penetration peg emerges. This acts to scaffold and reorganize the F-actin cytoskeleton and as a partitioning diffusion barrier to localize Bin-Amphiphysin-Rvs (BAR)-domain proteins, implicated in membrane curvature and protrusion of the penetration peg through the rice leaf surface (13).

In this report, we show that NADPH oxidases play distinct, but essential, roles in F-actin remodeling during plant infection. The Nox2 complex, which includes the $p67^{phox}$-like regulator NoxR, is necessary for assembly of septin GTPases at the appressorium pore, which is required for reorientation of the F-actin cytoskeleton at the point of plant infection. Consistent with this, Δ*nox2* mutants are unable to initiate penetration peg formation and cannot infect rice plants. We also show that Nox1 is required for correct organization of the toroidal F-actin network, acting after septin assembly. Δ*nox1* mutants therefore initiate penetration peg development but fail to elongate invasive hyphae to rupture the rice cuticle. These functions seem to require the regulated synthesis of ROS and are likely to be a direct consequence of the enzymatic activity of NADPH oxidases. Our results provide evidence that Nox complexes play critical roles in both initiation and maintenance of polarized growth by the rice blast fungus during plant infection.

Results

***M. oryzae* NADPH Oxidase Mutants Are Impaired in F-Actin Organization During Appressorium Development.** To understand the role of NADPH oxidases during infection-associated development, we identified *M. oryzae NOXR* (MGG_05280.6), which shares 38% amino acid sequence similarity with *Homo sapiens* $p67^{phox}$ (Fig. S1) and generated a Δ*noxR* null mutant (Fig. S2). We then introduced a LifeAct-RFP gene fusion (14) into isogenic *M. oryzae* Δ*nox1,* Δ*nox2*, Δ*nox1*Δ*nox2* (15), and Δ*noxR* mutants to observe organization of F-actin by live-cell imaging (13, 14). In the wild-type *M. oryzae* strain, Guy11, a large toroidal-shaped F-actin network (~5.9 μm in diameter) formed around the appressorium pore (13), which we visualized by live-cell imaging and topologically characterized using transverse line scan analysis of LifeAct-RFP fluorescence intensity in the appressorium (Fig. 1*A* and Movie S1). In Δ*nox1* mutants, the F-actin network was partially disorganized (Fig. 1 and Fig. S3 and Movie S2). Individual actin cables were not observed and a dense, unorganized patch of actin instead accumulated at the appressorium pore (2.5 ± 0.4 μm in diameter, $n = 20$). In the Δ*nox2* mutant, F-actin accumulated at the appressorium pore in a dense, unorganized patch (3.8 ± 0.3 μm in diameter, $n = 20$), shown in Fig. 1*A* and Movie S3. A similar pattern was observed in both the Δ*nox1*Δ*nox2* double mutant and in a Δ*noxR* mutant (4.2 ± 0.4 μm in diameter,

Author contributions: L.S.R., Y.F.D., Z.W., and N.J.T. designed research; L.S.R., Y.F.D., T.A.M., C.R.T., J.C., and Z.W. performed research; T.A.M., M.J.K., C.R.T., M.S., and J.C. contributed new reagents/analytic tools; L.S.R., Y.F.D., M.J.K., C.R.T., M.S., J.C., Z.W., and N.J.T. analyzed data; and L.S.R., C.R.T., and N.J.T. wrote the paper.

The authors declare no conflict of interest.

This article is a PNAS Direct Submission.

[1]To whom correspondence should be addressed. E-mail: N.J.Talbot@exeter.ac.uk.

This article contains supporting information online at www.pnas.org/lookup/suppl/doi:10.1073/pnas.1217470110/-/DCSupplemental.

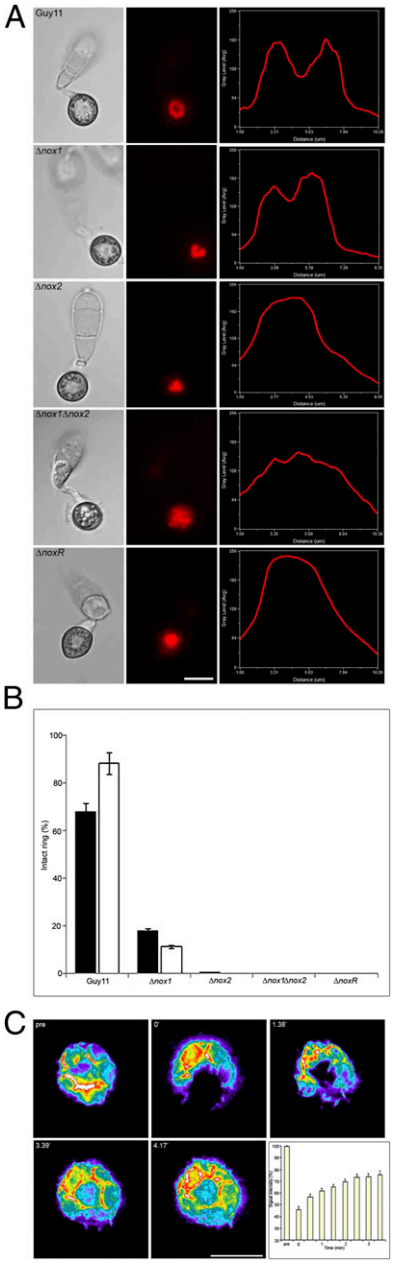

Fig. 1. *M. oryzae* NADPH oxidase mutants show aberrant F-actin organization during appressorium development. (*A*) Micrographs of F-actin organization visualized by expression of LifeAct-RFP in Guy11, Δ*nox1*, Δ*nox2*, Δ*nox1*Δ*nox2*, and Δ*noxR* mutants. Conidial suspensions at 5×10^4 mL^{-1} were inoculated onto glass coverslips for 24 h. Linescan graphs show LifeAct-RFP fluorescence in a transverse section of individual appressoria. (Scale bar, 10 μm.) (*B*) Bar chart to show percentage of appressoria containing intact F-actin rings after 16 h (black bars) and 24 h (white bars). Values are mean ±2 SE for three repetitions of the experiment, $n = 100$. (*C*) Recovery of LifeAct-RFP ring after partial photobleaching, with 75% recovery in fluorescence after 3.5 min. Values are means ±2 SE, $n = 24$). (Scale bar, 5 μm.)

$n = 20$), where a dense, unorganized patch of actin was located at the appressorium pore (Fig. 1 and Fig. S3 and Movies S4 and S5). To understand the nature of the F-actin network, we investigated fluorescence recovery of LifeAct-RFP after partial photobleaching. We found 75% recovery of fluorescence after 3.5 min, consistent with the appressorium F-actin toroidal network's being highly dynamic (Fig.1*C* and Movie S6). We conclude that F-actin organization at the appressorium pore in *M. oryzae* requires Nox1, Nox2, and NoxR.

To investigate why Nox1 and Nox2/NoxR seem to play distinct roles in F-actin organization during appressorium maturation, we decided to express Nox1-GFP, Nox2-RFP, and GFP-NoxR gene fusions in *M. oryzae* (Fig. S4 *A* and *B*). Nox1-GFP was predominantly localized at the plasma membrane during appressorium maturation (4–8 h), with evidence for subsequent endocytosis and internalization apparent at later times. By contrast, Nox2-RFP was initially found at the appressorium cortex (4 h) but was predominantly intracellular during appressorium maturation (8–12 h) and during cuticle penetration (Fig. S4*B*). Nox2-RFP was observed in intracellular vesicles throughout appressorium maturation. GFP-NoxR also showed intracellular localization with accumulation in the cytoplasm and vesicles. Transcriptional profile analysis showed distinct patterns of gene expression, with *NOX2* and *NOXR* genes showing much higher relative levels of expression during appressorium maturation (Fig. S4*C*). We conclude that Nox1 and Nox2/NoxR act at different subcellular locations during appressorium morphogenesis.

Nox2 Is Essential for Septin Ring Assembly at the Appressorial Pore. We reasoned that Nox1 and Nox2 might act in distinct ways to regulate F-actin assembly and organization and decided to test this idea. In *M. oryzae*, four septin GTPases (Sep3, Sep4, Sep5, and Sep6) are known to form a hetero-oligomeric ring at the appressorium pore (~5.9 μm in diameter) (13), which is necessary for F-actin organization. We therefore expressed Sep5-GFP in Δ*nox1,* Δ*nox2* Δ*nox1*Δ*nox2*, and Δ*noxR* mutants. In Guy11 and the Δ*nox1* mutant, a Sep5-GFP septin ring was present at the appressorium pore (Fig. 2*A*). In the Δ*nox2* mutant, however, Sep5-GFP formed a disorganized mass in the infection cell (3.2 ± 0.3 μm in diameter, $n = 20$; $P < 0.05$ compared with wildtype) (Fig. S5), which was also observed in a Δ*nox1*Δ*nox2* mutant (3.5 ± 0.6 μm in diameter, $n = 20$; $P < 0.05$) (Fig. 2*A*). In

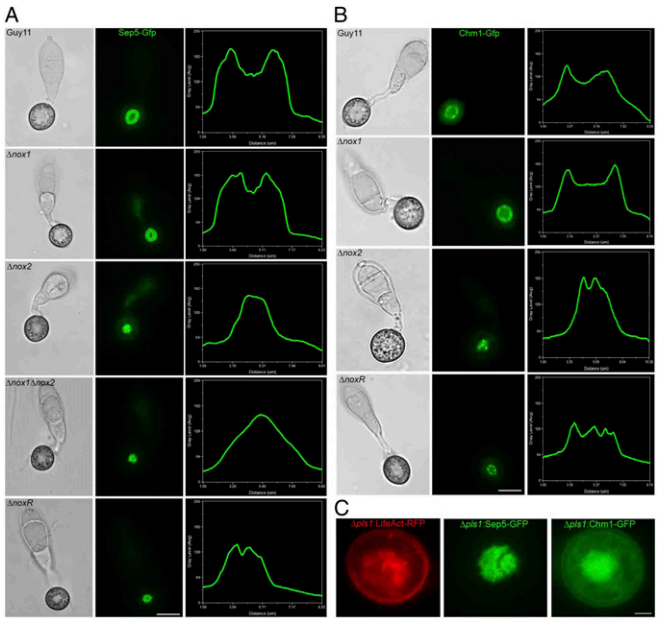

Fig. 2. *M. oryzae* Nox2 is essential for septin ring formation at the appressorium pore. (*A*) Micrographs to show cellular localization of Sep5-GFP in Guy11, Δ*nox1*, Δ*nox2*, Δ*nox1*Δ*nox2*, and Δ*noxR* during appressorium development after 24 h. Linescan graphs represent Sep5-GFP fluorescence in a transverse section of individual appressoria. (*B*) Micrographs to show localization of the Chm1 septin kinase in appressoria. Chm1-GFP was expressed in Guy11, Δ*nox1*, Δ*nox2*, and Δ*noxR* mutants. Linescan graphs showing Chm1-GFP fluorescence. (*C*) Micrographs to show localization of LifeAct-RFP, Sep5-GFP, and Chm1-GFP in the tetraspanin mutant Δ*pls1*. (Scale bars, 10 μm.)

Δ*noxR* mutants, aberrant septin rings formed, which were 19% smaller in diameter (mean = 4.76 μm, n = 20) than Sep5-GFP rings in Guy11 (Fig. 2). We also expressed a Chm1-GFP fusion in each of the Nox mutants. Chm1 is a protein kinase that in yeast is known to phosphorylate septins (16) and in *M. oryzae* is distributed in a ring conformation around the appressorium pore (14) (Fig. 2*B*). A Chm1-GFP ring was present in Guy11 and Δ*nox1* mutants but disorganized in Δ*nox2* and Δ*noxR* mutants, consistent with a role for Nox2 in the regulation of septin assembly and Chm1 kinase localization (Fig. 2*B*). Quantitative analysis confirmed that Nox2 is essential for septin and Chm1 ring assembly, showing more severe disruption of septin ring assembly than Δ*nox1* or Δ*noxR* mutants (Fig. S6 *A* and *B*). The *N*-WASP protein Las17, a component of the actin-polymerizing Arp2/3 complex, was observed by expression of a Las17-GFP fusion and localized as puncta in the appressorium pore in Guy11 (13) and the Δ*nox1* mutant, whereas in Δ*nox2* and Δ*noxR* mutants Las17-GFP localization was disrupted, with the protein distributed diffusely in the cytoplasm and plasma membrane (Fig S7). The ERM domain fusion protein Tea1-GFP, which localises as a ring of puncta at the appressorium pore in both Guy11 (13) and Δ*nox1* mutants, also showed abnormal localization in both Δ*nox2* and Δ*noxR* mutants. The localization of Rvs167-GFP, a BAR-domain protein (13), was also affected in Δ*nox2* and Δ*noxR* mutants, with puncta present in a misshapen appressorium pore (Fig. S7). We conclude that ERM–actin interactions at the appressorium pore, which are essential for linking cortical F-actin to the membrane to facilitate penetration peg emergence, require the Nox2/NoxR complex. Furthermore, the role of septins in spatially localizing the WASP/Arp2/3 complex component Las17 and BAR-domain protein Rvs167 to the appressorium pore—which mediate penetration peg emergence —is compromised in the absence of Nox2/NoxR.

Given the distinct function of Nox2 in regulating septin-mediated F-actin reorganization, we were interested in identifying other potential components of the Nox2 complex that might be involved in its recruitment to the appressorium pore. Studies in *M. oryzae, Podospora anserina*, and *Botrytis cinerea* have highlighted a connection between Nox2 (NoxB) and the transmembrane tetraspanin protein, Pls1 (17–19). Mutants lacking *PLS1* in these fungi strongly resemble *nox2* (*noxB*) mutants, and there is a very close phylogenetic association between fungi possessing both Nox2 and Pls1 homologs (20). It has been proposed that Pls1 might therefore be associated with Nox2 activity or specific recruitment to its site of action (21). To test this idea, we therefore expressed LifeAct-RFP, Sep5-GFP, and Chm1-GFP in a *M. oryzae* Δ*pls1* mutant (Fig. 2*C*). Strikingly, we observed mislocalization of F-actin, septin, and Chm1 in the absence of the Pls1 tetraspanin in the same manner as Δ*nox2* mutants.

Reactive Oxygen Species-Dependent Organization of the F-Actin Regulator Gelsolin in *M. oryzae*. We were interested in determining whether Nox-dependent cytoskeletal remodeling was due to regulated synthesis of ROS or a more indirect role in cell signaling. In mammalian systems, an increasing body of evidence suggests that ROS generation may affect F-actin dynamics during cell shape changes, migration, and cell motility (22), for example, in human sperm (23), low-density lipoprotein-induced stress fiber formation (24), endothelial cell mitogenesis, and during apoptosis (25). Antioxidants have been reported to exert a direct effect on F-actin cable elongation (26), and components of Nox complexes are also known to associate with F-actin (27) or actin-binding proteins (28). The actin-binding protein gelsolin, which regulates F-actin dynamics by uncapping free barbed ends to promote actin polymerization and by severing existing filaments (29), has, for example, been proposed as a likely target for regulation by ROS (22). We therefore expressed gelsolin-GFP in an *M. oryzae* Guy11 strain expressing LifeAct-RFP. We observed colocalization of gelsolin-GFP and LifeAct-RFP to the appressorium pore (Fig. 3*A*), consistent with gelsolin acting as an F-

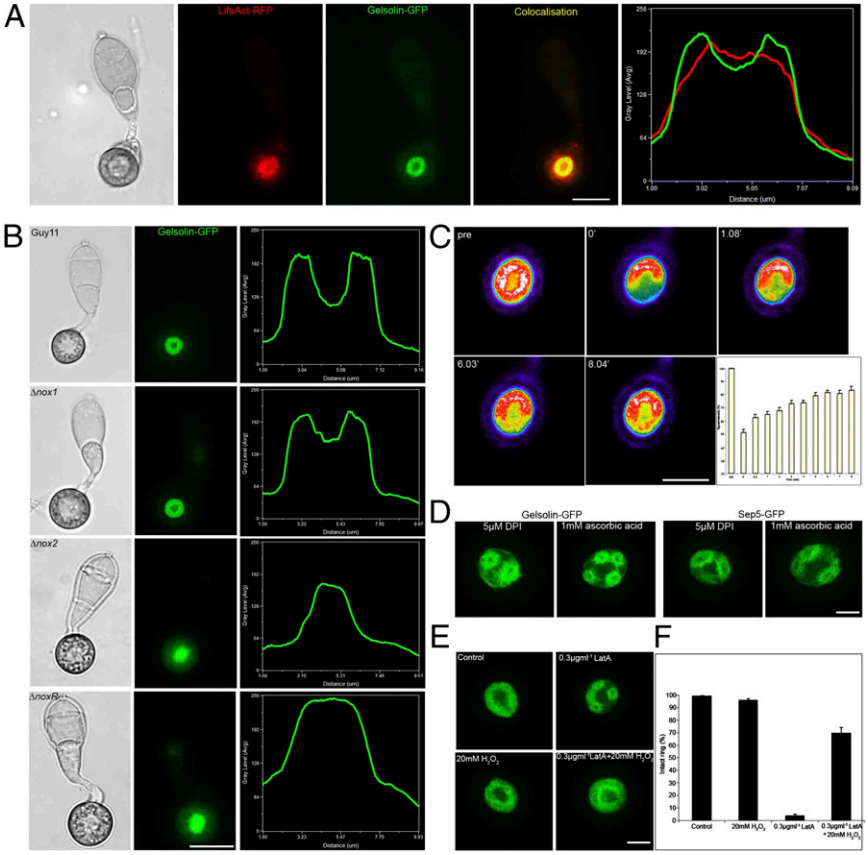

Fig. 3. Reactive oxygen species-dependent organization of the F-actin regulator, gelsolin, in *M. oryzae*. (*A*) Micrographs and linescan graph showing colocalization of LifeAct-RFP and gelsolin-GFP in the appressorium of the *M. oryzae* wild-type strain Guy11. (*B*) Micrographs and corresponding linescan graphs to show organization of gelsolin-GFP expressed in appressoria of Guy11, Δ*nox1*, Δ*nox2*, and Δ*noxR* mutants after 24 h. (*C*) Recovery of gelsolin-GFP ring after partial photobleaching, with 83% recovery after 8 min. Values are means ±2 SE, n = 23. (Scale bar, 5 μm.) (*D*) Micrographs to show effect of exposure to the NADPH oxidase inhibitor diphenylene iodonium (DPI) or antioxidant ascorbate on gelsolin-GFP and Sep5-GFP organization. Conidia expressing gelsolin-GFP and Sep5-GFP were independently exposed to 5 μM DPI or 1 mM ascorbic acid after 16 h and observed by epifluorescence microscopy after 24 h. (*E*) Micrographs to show effect of latrunculin A treatment on gelsolin-GFP organization in the presence or absence of ROS. Gelsolin-GFP was organized as a ring in *M. oryzae* in the presence or absence of 20 mM H_2O_2. Treatment with 0.3 μg/mL latrunculin A led to disorganization of gelsolin-GFP, which was partially remediated by simultaneous addition of 20 mM H_2O_2. (*F*) Bar chart showing percentage of appressoria containing intact gelsolin-GFP rings after 24 h. Values are means ±2 SE for three repetitions of the experiment, n = 50. (Scale bars, 10 μm.)

actin regulator. In a Δ*nox1* mutant, gelsolin-GFP still organized into a ring structure, but in Δ*nox2* or Δ*noxR* mutants gelsolin-GFP formed a disorganized patch at the appressorium base (Fig. 3*B*). To understand the nature of the gelsolin ring, we investigated fluorescence recovery after partial photobleaching. We found 83% recovery of fluorescence after 8 min, consistent with gelsolin turnover's being associated with F-actin dynamics (Fig. 3*C* and Movie S7). To determine whether F-actin and septin dynamics in appressoria were directly influenced by ROS synthesis, we applied the flavoenzyme (Nox) inhibitor diphenyleneiodonium chloride (15) and the antioxidant ascorbate, both of which prevented formation of gelsolin-GFP and septin rings, resulting instead in aberrant smaller ring structures at the appressorium pore (Fig. 3*D*). This is consistent with ROS generation's being required for both F-actin and septin ring assembly. We therefore applied the actin de-polymerizing agent latrunculin A to *M. oryzae* appressoria, which (as expected) led to disruption of gelsolin-GFP organization. However, when we applied hydrogen peroxide (H_2O_2) in the presence of latrunculin A, this partially restored gelsolin-GFP ring formation (Fig. 3 *E* and *F*). The depolymerizing activity of latrunculin A can therefore be partially prevented by the presence of high concentrations of ROS. Latrunculin A treatment of mature appressoria (at 16 h) also inhibited appressorium-mediated cuticle penetration on rice epidermal strips (Fig. S8), but this was partially remediated by simultaneous addition of H_2O_2 (Fig. S9). We conclude that regulated synthesis of ROS by *M. oryzae* Nox proteins can directly affect F-actin dynamics.

Nox1 and Nox2 Play Distinct Roles During Plant Infection. Given the distinct phenotypes of Δ*nox1* and Δ*nox2* mutants with respect to F-actin and septin dynamics, we were interested to see how they differed in their ability to cause rice blast disease. Previously, Δ*nox1* and Δ*nox2* mutants have been shown to be nonpathogenic (15), and we confirmed that Δ*noxR* and Δ*nox1*Δ*nox2* mutants were also unable to cause rice blast disease (Fig. 4*A*). Transmission electron microscopy of appressoria, however, showed that Δ*nox1* mutants still initiated penetration peg formation from the base of the infection cell (Fig. 4*C*). These short projections were unable to extend through the plant cell wall (Fig. 4*B*) and Δ*nox1* mutants were therefore unable to colonize rice tissue and cause disease. By contrast, appressoria of Δ*nox2*, Δ*nox1*Δ*nox2*, and Δ*noxR* mutants were unable to repolarize at the appressorium pore and could not form penetration pegs (Fig. 4 *D–F*). We conclude that Nox2 and NoxR are necessary for septin-mediated initiation of polarized growth of the penetration peg at the appressorium base, whereas Nox1 is necessary for maintenance of penetration peg elongation.

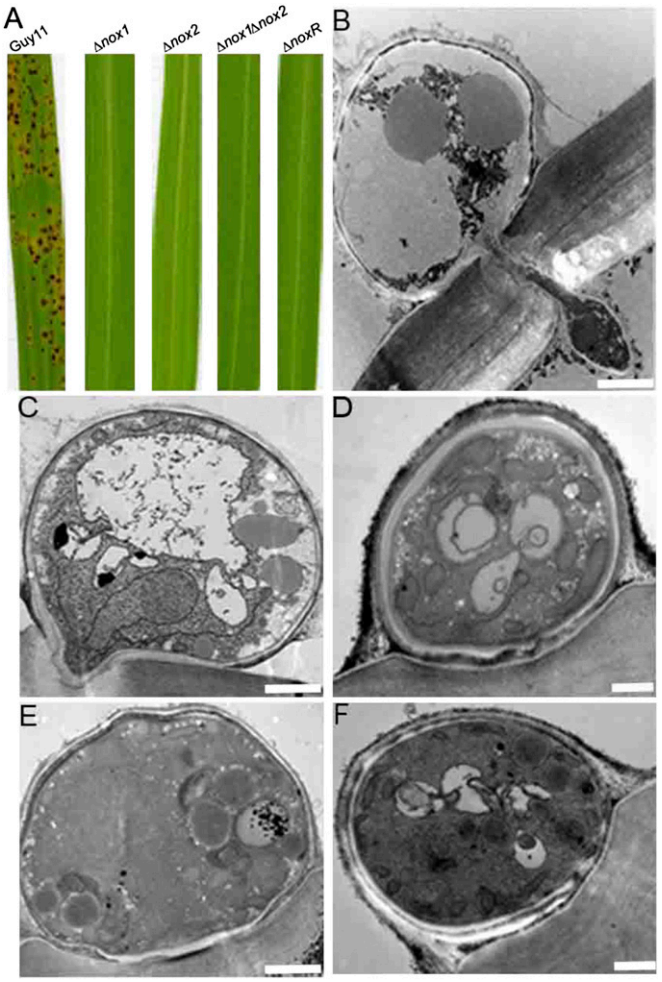

Fig. 4. *M. oryzae* NADPH oxidase mutants do not cause rice blast disease. (*A*) Seedlings of rice cultivar CO-39 were inoculated with *M. oryzae* conidial suspensions of equal concentration (1×10^5 conidia/mL) of wild-type Guy11 and isogenic Δ*nox1*, Δ*nox2*, Δ*nox1*Δ*nox2*, and Δ*noxR* mutants. Seedlings were incubated for 5 d to allow development of blast disease symptoms. (*B–F*) Transmission electron micrographs showing transverse sections of appressoria undergoing development on onion epidermis after 24 h. (*B*) Guy11 appressorium showing penetration hypha development. (*C*) Δ*nox1* mutant appressorium showing repolarization to form an aberrant penetration peg. (*D*) Δ*nox2* mutant appressorium impaired in penetration peg development. (*E*) Δ*nox1*Δ*nox2* mutant. (*F*) Δ*noxR* mutant. (Scale bars, 2.0 μm.)

Discussion

Regulated synthesis of ROS by NADPH oxidases is necessary for a wide variety of developmental processes in mammals, plants, and fungi (1, 3, 6). In filamentous fungi, ROS generation has, for example, been associated with hyphal tip growth, spore formation, infection structure development, conidial anastomosis tube generation, fruiting body formation, fungal–plant mutualistic interactions, and fungal virulence (1, 2). These diverse roles for ROS as signaling molecules in fungi are, however, still not well understood. The best understood NADPH oxidase is the mammalian phagocytic leukocyte $gp91^{phox}$ (or Nox2), which is necessary for the defensive oxidative burst during microbial attack. The $gp91^{phox}$ protein is part of a membrane-spanning complex (flavocytochrome b_{558}) with the adaptor protein $p22^{phox}$ and interacts with the cytosolic regulatory proteins $p40^{phox}$, $p67^{phox}$, $p47^{phox}$, and Rac GTPase (3). In total there are five Nox enzymes in humans, which have been implicated in a variety of cellular processes, including cell proliferation, apoptosis, and hormone responses. This has led to the suggestion that ROS production may be a ubiquitous signaling system controlling cellular differentiation in eukaryotes (3–6). Filamentous fungi possess up to three Nox enzymes. Nox 1 (or NoxA) and Nox2 (NoxB) are similar to $gp91^{phox}$, whereas Nox3 (NoxC) enzymes have EF-hand domains that putatively bind Ca^{2+} in the same way as plant respiratory burst oxidases (8, 9) and human Nox5 (3). Fungal Nox complexes seem to involve interactions with cytosolic proteins, previously implicated in the regulation of polarity (1). A recent study of the plant-associated mutualistic fungus *Epichloë festucae*, for example, showed that NoxR interacts with homologs of the yeast polarity proteins Bem1 and Cdc24 (2) and that this requires the Phox and Bem1 (PB1) protein domain, which is also necessary for localization of these proteins to actively growing hyphal tips. *E. festucae* mutants that lack Bem1 are defective in hyphal morphogenesis and growth in culture whereas Cdc24 seems to be essential for viability (2). The study therefore provided evidence for an important role for fungal NADPH oxidases in the establishment of polarity and the control of cellular differentiation. This is consistent with recent findings in plant pathogenic fungi, such as *Botrytis cinerea*, *Sclerotinia sclerotiorum*, and *Claviceps purpurea*, in which Nox proteins have been shown to be necessary for fruit body formation and appressorium function (1, 25, 26),

and experiments in *Podospora anserina* that have implicated Nox proteins in polarity establishment and invasive growth (27).

In this report, we have provided evidence that the role of fungal Nox in polarized fungal growth is likely to be based on remodeling of the F-actin cytoskeleton. When considered together, our results are consistent with a model whereby the *M. oryzae* Nox2/NoxR complex is essential for septin-mediated F-actin assembly at the appressorium pore, which is a prerequisite for penetration peg formation and rice infection. In *Saccharomyces cerevisiae,* a recently identified Nox-encoding gene, *YNO1*, has also been implicated in actin cable formation (30), suggesting that regulation of F-actin dynamics may be one of the key underlying mechanisms by which Nox exert their diverse roles in cellular differentiation. In *M. oryzae*, Nox2 is regulated as part of a complex involving NoxR and is also known to interact with Rac1 (31), a small GTPase involved in polarized cell growth and also implicated in F-actin dynamics. Gelsolin is, for instance, a downstream effector of Rac1 (32). We also found evidence that the tetraspanin Pls1 may play a role in the Nox2 complex based on its effect on septin and F-actin organization at the appressorium pore. Nox2 is therefore essential for initiation of polarized growth from the appressorium. Remediation of the effects of the actin depolymerizing agent latrunculin A upon exposure to H_2O_2, furthermore, suggests that the role of Nox2 and NoxR in polarity establishment may be a direct consequence of the regulated synthesis of ROS by NADPH oxidases, perhaps acting directly on actin regulatory proteins such as gelsolin. It has been suggested, for instance, that ROS may increase the actin-severing ability of gelsolin by disulfide bond formation in the protein, leading to greater exposure of barbed ends and increased actin polymerization (22).

By contrast, we found that Nox1 is not required for septin ring assembly at the appressorium pore but is necessary for correct organization of the F-actin network that is scaffolded at this site. Furthermore, Δ*nox1* mutants are able to initiate penetration peg formation (and therefore establish polarized growth) but cannot elongate invasive hyphae, suggesting that the Nox1 complex may be required for maintenance of polarized growth, which is necessary for host cell entry and pathogenesis. Previously, it was shown that Δ*nox1* mutants display increased resistance to calcofluor white, indicating a defect in cell-wall organization affecting chitin deposition. The lighter pigmentation of Δ*nox1* mutants also suggests a role in melanin biosynthesis or its polymerization in the cell wall. These phenotypes are notably absent in the other Nox mutants, suggesting that Nox1 may supply ROS to the cell wall for oxidative cross-linking of proteins, and this may be necessary for maintenance of polarized growth.

An important question that arises from this study is how two Nox complexes in the *M. oryzae* appressorium, which are likely to involve the same $p67^{phox}$ regulator, NoxR, can fulfill different functions. Our observations suggest that specificity may be due, at least in part, to their distinct subcellular locations. Nox1 occurs predominantly in the plasma membrane, resulting in extracellular ROS generation and consistent with its role in cell wall organization. Conversely, Nox2 is present intracellularly and is differentially expressed during appressorium maturation. Localization of Nox2 within membrane-bound vesicles is similar to localization patterns of NoxA and NoxB to the endoplasmic reticulum (ER) observed in *B. cinerea* (21). Furthermore, Yno1 in yeast (30) and mammalian Nox4 also localize to the ER, suggesting that this may be an important site to ROS generation (21). Although we have not yet verified whether Nox2 acts within the ER, its intracellular location and association with the Pls1 tetraspanin suggests that it does act in a very different manner from Nox1, generating ROS within the appressorium to regulate F-actin organization.

We conclude that infection of rice cells by *M. oryzae* therefore involves two separately operating Nox complexes that regulate the establishment of polarized growth by septin-mediated reorganization of F-actin at the appressorium pore and then maintain polarized growth of the penetration hypha and organization of cortical F-actin. These findings offer a potential target for rice blast disease control and, importantly, they may also provide insight into the action of NADPH oxidases in diverse developmental processes in fungi, plants and animals.

Materials and Methods

Fungal Strains, Growth Conditions, and DNA Analysis. The growth and maintenance of *M. oryzae* isolate, media composition, nucleic acid extraction, and fungal transformation were all as previously described (33). Gel electrophoresis, restriction enzyme digestion, gel blots, and sequencing were performed using standard procedures (34).

Plant Infection Assays. Pathogenicity assays were performed by spraying seedlings of rice (*Oryza sativa*) cultivar CO-39 with a suspension of 10^5 conidia/mL using an artist's airbrush (33). Infection-related development was observed by incubating conidia on hydrophobic glass coverslips and allowing appressoria to form after 24 h. Cuticle penetration was measured as described ref. 35.

Generation of *M. oryzae* Δ*noxR* Mutant and Strains Expressing GFP Fusions. Targeted gene replacement of the *NOXR* encoding gene was performed using the split-marker strategy. Vectors were constructed using a Hygromycin B-selectable marker, *hph*, for transformation of Guy11. The *hph* gene cassette was cloned into pBluescript (Stratagene) as a 1.4-kb EcoRI–XbaI fragment. To amplify the split *hph* templates the primers used were M13 F with HY and M13 R with YG, as described previously (36). *M. oryzae NOXR* was amplified using primers designed to conserved DNA regions identified from an alignment of noxR sequences from *M. oryzae*, *E. festucae*, and *H. sapiens* (Table S1). The noxR sequence was retrieved from the *M. oryzae* genome database of the Broad Institute at the Massachussetts Institute of Technology, Cambridge, MA (www.broad.mit.edu/annotation/fungi/magnaporthe). The wild-type Guy11 was transformed with the *noxR:hph* deletion cassette. Transformants were selected in the presence of hygromycin B (200 μg/mL) and assessed by Southern blot analysis. For generation of translational GFP fusions, GAP repair cloning based on homologous recombination in *Saccharomyces cerevisiae* was used (37). Primers used are listed in Table S1. All translational GFP fusions were created using the native promoter and terminator sequences. Plasmids were transformed into Guy11, Δ*nox1*, Δ*nox2*, Δ*noxR*, or Δ*pls1* strains and single-copy transformants selected by Southern blot.

Analysis of Gene Expression Using High-Throughput SuperSAGE. A transcriptional profiling database (http://cogeme.ex.ac.uk/supersage/) (38) was interrogated to determine the expression of *NOX1*, *NOX2*, and *NOXR* in Guy11 during appressorium development (4, 6, 8, 14, and 16 h after spore germination). Expression was plotted relative to gene expression in *M. oryzae* mycelium (38).

Light and Epifluorescence Microscopy and Transmission Electron Microscopy. For epifluorescence microscopy conidia were incubated on coverslips/leaf sheath and observed at each time point using an IX-81 Olympus inverted microscope connected to a CoolSNAP HQ2 camera. Photobleaching experiments were performed using a IX-81 Olympus inverted microscope with VS-LMS4 Laser-Merge-System and solid-state lasers (488 nm/70 mW and 561 nm/70 mW; Visitron Systems) and a PlanApo 100×/NA 1.45 Oil TIRF objective (Olympus). The 405-nm/60-mW diode laser was modified by use of a ND 0.6 filter, resulting in 15 mW of output power coupled into the light path by an OSI-IX 71 adaptor (Visitron Systems) and controlled by a UGA-40 controller (Rapp OptoElectronic GmbH) and VisiFRAP 2D FRAP control software for Meta Series 7.5.× (Visitron Systems). For recovery curves, part of the Life-act-RFP or Gelsolin-GFP ring was photobleached and the average intensity of the region was measured and normalized with an unbleached region of the ring. Three-dimensional projections were captured using a Zeiss LSM510 Meta confocal laser scanning microscope system. HeNe 543-nm lasers were used for excitation, and all images were recorded following examination under the 363× oil objective. LSM image browser (Zeiss) or Metamorph 7.5 (molecular devices) was used for image analysis. Ultra-thin sectioning and transmission electron microscopy was performed as described previously (15).

ACKNOWLEDGMENTS. This work was supported by Grant BB/G013896/ from the Biotechnology and Biological Sciences Research Council (to N.J.T. and C.R.T.), Grant 31030004 from the National Natural Science Foundation of China (to J.C. and Z.W.), a Halpin Scholarship (to Y.F.D.), and a European Research Council Advanced Investigator award (to N.J.T.).

1. Sumimoto H (2008) Structure, regulation and evolution of Nox-family NADPH oxidases that produce reactive oxygen species. *FEBS J* 275(13):3249–3277.
2. Lambeth JD (2004) NOX enzymes and the biology of reactive oxygen. *Nat Rev Immunol* 4(3):181–189.
3. Brown DI, Griendling KK (2009) Nox proteins in signal transduction. *Free Radic Biol Med* 47(9):1239–1253.
4. Suzuki N, et al. (2011) Respiratory burst oxidases: The engines of ROS signaling. *Curr Opin Plant Biol* 14(6):691–699.
5. Torres MA, Dangl JL, Jones JD (2002) Arabidopsis gp91phox homologues AtrbohD and AtrbohF are required for accumulation of reactive oxygen intermediates in the plant defense response. *Proc Natl Acad Sci USA* 99(1):517–522.
6. Foreman J, et al. (2003) Reactive oxygen species produced by NADPH oxidase regulate plant cell growth. *Nature* 422(6930):442–446.
7. Heller J, Tudzynski P (2011) Reactive oxygen species in phytopathogenic fungi: Signaling, development, and disease. *Annu Rev Phytopathol* 49:369–390.
8. Takemoto D, et al. (2011) Polarity proteins Bem1 and Cdc24 are components of the filamentous fungal NADPH oxidase complex. *Proc Natl Acad Sci USA* 108(7): 2861–2866.
9. Takemoto D, Tanaka A, Scott B (2007) NADPH oxidases in fungi: Diverse roles of reactive oxygen species in fungal cellular differentiation. *Fungal Genet Biol* 44(11): 1065–1076.
10. Wilson RA, Talbot NJ (2009) Under pressure: Investigating the biology of plant infection by Magnaporthe oryzae. *Nat Rev Microbiol* 7(3):185–195.
11. Fisher MC, et al. (2012) Emerging fungal threats to animal, plant and ecosystem health. *Nature* 484(7393):186–194.
12. de Jong JC, McCormack BJ, Smirnoff N, Talbot NJ (1997) Glycerol generates turgor in rice blast. *Nature* 389:244–244.
13. Dagdas YF, et al. (2012) Septin-mediated plant cell invasion by the rice blast fungus, Magnaporthe oryzae. *Science* 336(6088):1590–1595.
14. Berepiki A, Lichius A, Read ND (2011) Actin organization and dynamics in filamentous fungi. *Nat Rev Microbiol* 9(12):876–887.
15. Egan MJ, Wang ZY, Jones MA, Smirnoff N, Talbot NJ (2007) Generation of reactive oxygen species by fungal NADPH oxidases is required for rice blast disease. *Proc Natl Acad Sci USA* 104(28):11772–11777.
16. Versele M, Thorner J (2004) Septin collar formation in budding yeast requires GTP binding and direct phosphorylation by the PAK, Cla4. *J Cell Biol* 164(5):701–715.
17. Clergeot PH, et al. (2001) PLS1, a gene encoding a tetraspanin-like protein, is required for penetration of rice leaf by the fungal pathogen Magnaporthe grisea. *Proc Natl Acad Sci USA* 98(12):6963–6968.
18. Gourgues M, Brunet-Simon A, Lebrun MH, Levis C (2004) The tetraspanin BcPls1 is required for appressorium-mediated penetration of Botrytis cinerea into host plant leaves. *Mol Microbiol* 51(3):619–629.
19. Lambou K, et al. (2008) The crucial role of the Pls1 tetraspanin during ascospore germination in Podospora anserina provides an example of the convergent evolution of morphogenetic processes in fungal plant pathogens and saprobes. *Eukaryot Cell* 7 (10):1809–1818.
20. Malagnac F, et al. (2008) Convergent evolution of morphogenetic processes in fungi: Role of tetraspanins and NADPH oxidases 2 in plant pathogens and saprobes. *Commun Integr Biol* 1(2):180–181.
21. Tudzynski P, Heller J, Siegmund U (2012) Reactive oxygen species generation in fungal development and pathogenesis. *Curr Opin Microbiol* 15(6):653–659.
22. Moldovan L, Mythreye K, Goldschmidt-Clermont PJ, Satterwhite LL (2006) Reactive oxygen species in vascular endothelial cell motility. Roles of NAD(P)H oxidase and Rac1. *Cardiovasc Res* 71(2):236–246.
23. de Lamirande E, Tsai C, Harakat A, Gagnon C (1998) Involvement of reactive oxygen species in human sperm arcosome reaction induced by A23187, lysophosphatidylcholine, and biological fluid ultrafiltrates. *J Androl* 19(5):585–594.
24. Holland JA, et al. (2001) Low-density lipoprotein induced actin cytoskeleton reorganization in endothelial cells: Mechanisms of action. *Endothelium* 8(2):117–135.
25. Irani K (2000) Oxidant signaling in vascular cell growth, death, and survival : A review of the roles of reactive oxygen species in smooth muscle and endothelial cell mitogenic and apoptotic signaling. *Circ Res* 87(3):179–183.
26. Pardee JD, Simpson PA, Stryer L, Spudich JA (1982) Actin filaments undergo limited subunit exchange in physiological salt conditions. *J Cell Biol* 94(2):316–324.
27. Tamura M, Kai T, Tsunawaki S, Lambeth JD, Kameda K (2000) Direct interaction of actin with p47(phox) of neutrophil NADPH oxidase. *Biochem Biophys Res Commun* 276(3):1186–1190.
28. Wientjes FB, Reeves EP, Soskic V, Furthmayr H, Segal AW (2001) The NADPH oxidase components p47(phox) and p40(phox) bind to moesin through their PX domain. *Biochem Biophys Res Commun* 289(2):382–388.
29. Kwiatkowski DJ (1999) Functions of gelsolin: Motility, signaling, apoptosis, cancer. *Curr Opin Cell Biol* 11(1):103–108.
30. Rinnerthaler M, et al. (2012) Yno1p/Aim14p, a NADPH-oxidase ortholog, controls extramitochondrial reactive oxygen species generation, apoptosis, and actin cable formation in yeast. *Proc Natl Acad Sci USA* 109(22):8658–8663.
31. Chen J, et al. (2008) Rac1 is required for pathogenicity and Chm1-dependent conidiogenesis in rice fungal pathogen Magnaporthe grisea. *PLoS Pathog* 4(11): e1000202.
32. Arcaro A (1998) The small GTP-binding protein Rac promotes the dissociation of gelsolin from actin filaments in neutrophils. *J Biol Chem* 273(2):805–813.
33. Talbot NJ, Ebbole DJ, Hamer JE (1993) Identification and characterization of MPG1, a gene involved in pathogenicity from the rice blast fungus Magnaporthe grisea. *Plant Cell* 5(11):1575–1590.
34. Sambrook J, Fritsch EF, Maniatis T (1989) *Molecular Cloning: A Laboratory Manual* (Cold Spring Harbour Laboratory Press, New York), 2nd Ed.
35. Thines E, Weber RW, Talbot NJ (2000) MAP kinase and protein kinase A-dependent mobilization of triacylglycerol and glycogen during appressorium turgor generation by Magnaporthe grisea. *Plant Cell* 12(9):1703–1718.
36. Kershaw MJ, Talbot NJ (2009) Genome-wide functional analysis reveals that infection-associated fungal autophagy is necessary for rice blast disease. *Proc Natl Acad Sci USA* 106(37):15967–15972.
37. Oldenburg KR, Vo KT, Michaelis S, Paddon C (1997) Recombination-mediated PCR-directed plasmid construction in vivo in yeast. *Nucleic Acids Res* 25(2):451–452.
38. Soanes DM, Chakrabarti A, Paszkiewicz KH, Dawe AL, Talbot NJ (2012) Genome-wide transcriptional profiling of appressorium development by the rice blast fungus *Magnaporthe oryzae*. *PLoS Pathog* 8(2):e1002514.